

Autopilot Spatially-Adaptive Active Contour Parameterization for Medical Image Segmentation

Eleftheria A. Mylona¹, Michalis A. Savelonas¹, Dimitris Maroulis¹, Athanassios N. Skodras²,

¹*Department of Informatics and Telecommunications, University of Athens, Greece*

²*Department of Electrical and Computer Engineering, University of Patras, Greece*

¹{emylona, msavel, dmaroulis}@di.uoa.gr

²skodras@upatras.gr

Abstract

In this work, a novel framework for automated, spatially-adaptive adjustment of active contour regularization and data fidelity parameters is proposed and applied for medical image segmentation. The proposed framework is tailored upon the isomorphism observed between these parameters and the eigenvalues of diffusion tensors. Since such eigenvalues reflect the diffusivity of edge regions, we embed this information in regularization and data fidelity parameters by means of entropy-based, spatially-adaptive ‘heatmaps’. The latter are able to repel an active contour from randomly directed edge regions and guide it towards structured ones. Experiments are conducted on endoscopic as well as mammographic images. The segmentation results demonstrate that the proposed framework bypasses iterations dedicated to false local minima associated with noise, artifacts and inhomogeneities, speeding up contour convergence, whereas it maintains a high segmentation quality.

1. Introduction

Across the field of active contour segmentation, nearly all models rely on parameters which need to be tuned on a trial and error basis [1]-[5]. Researchers propose contradictory claims for empirically optimized parameterization, dependent on each dataset to be tested. A generally applicable active contour parameter configuration is still an open issue.

Region-based active contours have been proposed in image analysis literature as suitable for several medical imaging modalities [6]-[9]. They are topologically adaptable and cope well with regions of weak edges, such as human tissues. Like most active contour models, they rely on parameters weighting the

so-called *regularization* and *data fidelity* energy terms, which significantly affect their performance. Despite this significance, in most existing methods, both regularization and data fidelity terms are manually set and kept intact over the image. As a result, segmentation results are suboptimal and subjective. In addition, manual parameter setting asks for technical skills from the end-user, who is very often a Medical Doctor (MD).

Tracing the state-of-the-art methods presented in literature trying to tackle the issue of region-based active contour empirical parameterization, two key elements are mainly considered: a) the trade-off between regularization and data fidelity terms as well as, b) the spatial variance of regularization and data fidelity parameters. Ma and Yu [10] try to solve the balance between energy terms by utilizing a morphological approach. However, their method does not adjust each individual parameter separately. McIntosh and Hamarneh [11] adapt regularization weights across a set of images. Although an optimal regularization weight can be found for a single image in a set, the same weight may not be optimal for all regions of that image. In addition, the data fidelity term is still empirically determined. Erdem and Tari [12] utilize data-driven local cues focusing on edge consistency and texture cues. Nevertheless, this method requires technical skills from the end user. Pluempitiwiriyaweg et al. [13] and Tsai et al. [14] update parameters during the iterative process of evolution. Nonetheless, this dependency may yield to the propagation of early errors in the latter stages of contour evolution. Dong et al. [15] attempt to vary the regularization term based on the surface curvature of a pre-segmented vessel. However, the regularization weight does not rely on image properties. On the contrary, it depends upon the shape of the target region thus, limiting the general applicability of the method on different image modalities.

In this work, a novel framework for automated, spatially-adaptive adjustment of regularization and data fidelity parameters of active contours is presented and applied for the segmentation of medical images. The proposed framework aims to relieve MDs from the tedious and time-consuming process of empirical parameterization of active contours, as well as to enrich segmentation results with objectivity and reproducibility, in order to support early diagnosis and clinical evaluation. It is based on the key observation that regularization and data fidelity parameters share the same orthogonal directions with the eigenvalues of diffusion tensors. These eigenvalues hold essential information associated with localized edges. Accordingly, we embed this information in the regularization and data fidelity parameters by means of entropy-based, spatially-adaptive ‘heatmaps’. The latter are able to drive the contour away from randomly directed edge regions and guide it towards structured ones. Hence, iterations dedicated to false local minima are bypassed, speeding up contour convergence. The proposed framework does not require technical skills from the end-user, is applicable to various medical image modalities and is not affected by alterations on the shape of target regions. In addition, due to its simplicity, it can be embedded into several region-based active contour variations.

The remainder of this paper is organized as follows: Section 2 presents the proposed framework and Section 3 demonstrates the experimental results. The conclusions of this study are summarized in Section 4.

2. Proposed framework

The proposed framework takes into account the concept of anisotropic diffusion patterns [16]. The latter allow the mapping of spatially-varying regions in accordance with their directionality. Fig. 1(a) depicts a schematic representation of this idea with several ellipsoids consisting of different diffusion patterns. Two of them correspond to a single direction and are thus associated with structured target edge regions, whereas the next two correspond to multiple directions and are therefore associated with noisy regions or regions of image artifacts. It should be mentioned that, medical images consist of target regions which exhibit weak edges however; these images are also plagued by artifacts and noise as well as heterogeneity which yields to inhomogeneous background.

Aiming at capturing the nature of each region in a medical image, i.e. whether it corresponds to a target edge or noisy region, the Information Entropy (*IE*) measure is utilized. The latter obtains high values

in cases of regions characterized by a diffusion pattern of multiple directions. On the contrary, entropy obtains lower values in cases of regions characterized by a diffusion pattern of one unique direction. Fig. 1(b) depicts the entropy behavior on each diffusion pattern of Fig. 1(a).

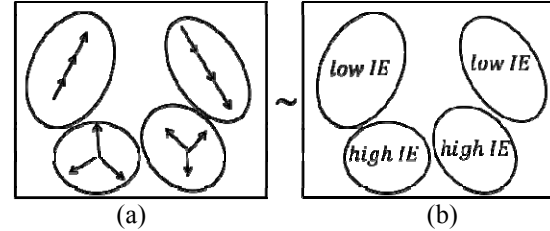


Figure 1. A schematic representation of distinct diffusion patterns, (a) ellipsoids consisting of single and multiple direction diffusion patterns, (b) entropy behavior *IE* on each diffusion pattern.

In the context of the proposed framework, the image is considered as a grid of $q \times q$ samples. The sample size must be sufficiently large to preserve the direction of the main structures of the target region. Each sample is decomposed to the finest and second finest scales by means of a multi-scale, multi-directional and anisotropic filtering descriptor such as the contourlet transform [17]. For each subband image I_{jk} , entropy measures are calculated according to the following equations:

$$IE_{jk} = -\sum_{n=1}^{N_{jk}} \sum_{m=1}^{M_{jk}} p_{jk}(m,n) \cdot \log p_{jk}(m,n) \quad (1)$$

$$p_{jk}(m,n) = \frac{|I_{jk}(m,n)|^2}{\sqrt{\sum_{n=1}^{N_{jk}} \sum_{m=1}^{M_{jk}} [I_{jk}(m,n)]^2}} \quad (2)$$

where IE_{jk} is the information entropy of the subband image I_{jk} in the k^{th} direction and the j^{th} level, M_{jk} is the row size and N_{jk} the column size of the subband image. As a result, spatially-adaptive entropy ‘heatmaps’ are formulated in order to reflect the diffusivity along each region.

Considering once more the diffusion patterns illustrated in Fig. 1(a), each ellipsoid is characterized by two axes, the principal and the minor, which describe its length and width, respectively and are perpendicular to each other. These axes correspond to principal and minor eigenvectors and eigenvalues. The principal eigenvalue λ_1 reflects the diffusivity along

the principal eigenvector and is longitudinal with respect to the principal axis, whereas the minor eigenvalue λ_2 reflects the diffusivity along the minor eigenvector and is vertical with respect to the principal axis. Fig. 2(a) depicts principal and minor eigenvalues of an ellipsoid.

Region-based active contours evolve by minimizing the following energy functional:

$$E = w_{reg} \cdot E_{reg} + w_{df} \cdot E_{df} \quad (3)$$

where E_{reg} and E_{df} are associated with regularization and data fidelity energy terms, respectively, whereas w_{reg} and w_{df} are weighting parameters.

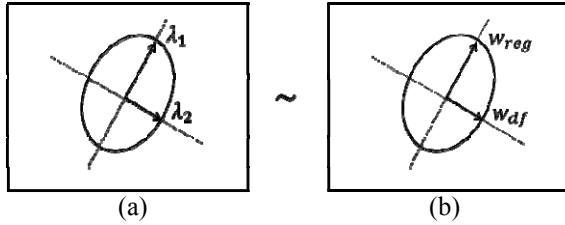


Figure 2.(a) Eigenvalues of ellipsoid, (b) regularization and data fidelity parameters of active contour.

Fig. 2(b) depicts regularization and data fidelity parameters of a contour. Regularization and data fidelity forces are tangent and vertical with respect to the principal axis of the contour, respectively. It is tempting to notice that the regularization weight corresponds to the same direction as the principal eigenvalue of the ellipsoid. This is also the case with the data fidelity weight, which corresponds to the same direction as the minor eigenvalue. This isomorphism indicates a link between the regularization and data fidelity parameters and the eigenvalues of diffusion patterns.

As eigenvalues reflect the diffusivity along the axes of an ellipsoid, regularization and data fidelity parameters reflect the diffusivity along the axes of the contour by means of spatially-adaptive entropy ‘heatmaps’ and are calculated according to the following equations:

$$w_{reg} \propto (1/w_{df}) \times N \times M, \quad w_{df} = \arg_{I_{jk}} \max(IE_{jk}(I_{jk})) \quad (4)$$

The key notion is that, by appropriately amplifying data fidelity forces in noisy, high-entropy regions, the contour will be repelled. Hence, iterations dedicated to erroneous local minima will be bypassed, speeding up contour convergence towards target edges. It should be noticed that the proposed framework achieves autopilot spatially-adaptive parameterization.

3. Results

The proposed framework has been integrated into the region-based Chan-Vese model [5] so as to evaluate the segmentation performance of the autopilot version versus the manually fine-tuned version. The experimental results are evaluated by means of the region overlap measure, known as the Tanimoto Coefficient (TC) [18], which is defined by:

$$TC = \frac{N(A \cap B)}{N(A \cup B)} \quad (5)$$

where A is the region identified by the segmentation method under evaluation, B is the ground truth region and $N()$ indicates the number of pixels of the enclosed region.

Experiments are conducted on two sets of medical images. The first set consists of 32 endoscopic images containing polyps, provided by the General Hospital of Athens ‘Laiko’, Medical School, University of Athens. All polyps were investigated by MD experts, who provided ground truth segmentations. Fig. 3 illustrates segmentation results of the autopilot Chan-Vese model, using the proposed framework.

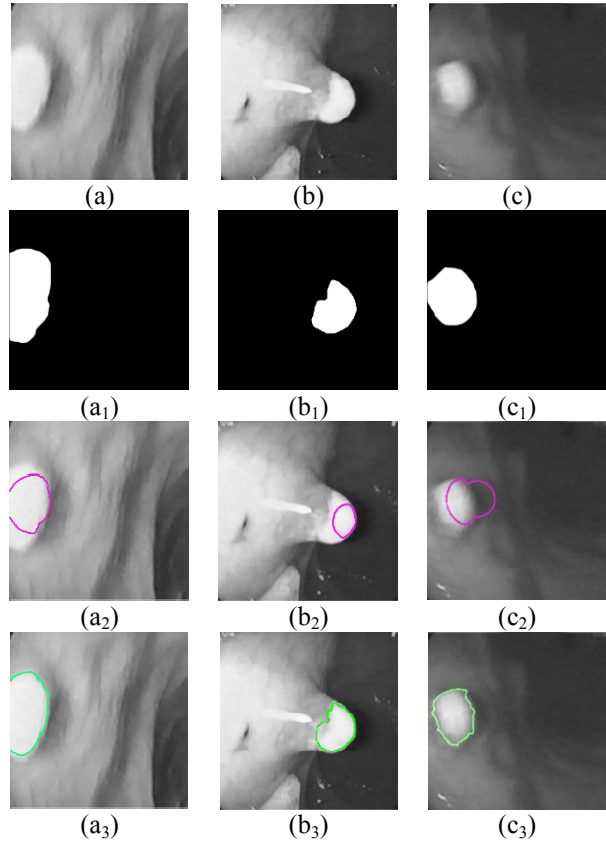


Figure 3.(a)-(c) Endoscopy images containing polyps, (a₁)-(c₁) ground truth images, (a₂)-(c₂) segmentations obtained by the manually fine-tuned version, in the same iteration that the autopilot version has converged, (a₃)-(c₃) segmentation results of the autopilot Chan-Vese model.

Leaned on the results it is evident that, in the manually fine-tuned version which utilizes fixed, spatially-uniform parameters, contour convergence is delayed. On the contrary, the results support the autopilot version, where forces guiding contour evolution are appropriately amplified in non-target, high-entropy regions, accelerating convergence.

The second set consists of 50 mammographic images randomly obtained by the Mini-MIAS Database [19] containing fatty, well-defined and ill-defined, benign and malignant masses. Fig. 4 illustrates segmentation results of the autopilot Chan-Vese model, using the proposed framework. It is once more evident that the autopilot version yields a high segmentation quality at a much reduced convergence rate.

The autopilot version achieves an average TC value of $82.9 \pm 1.6\%$, which is comparable to the TC value of $80.7 \pm 1.8\%$ obtained by the manually fine-tuned version, with regards to both endoscopic and mammographic images tested. However, the autopilot version converges in 10-20 times less iterations. The original version achieves a TC value of $52.4 \pm 11.3\%$, *in the same iteration that the autopilot version has converged*.

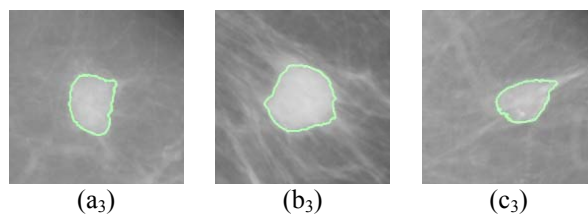
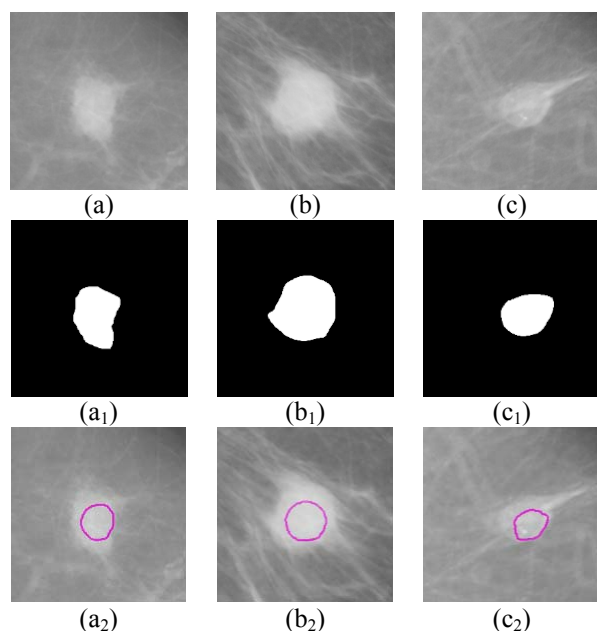


Figure 4.(a)-(c) Mammographic images containing abnormalities, (a₁)-(c₁) ground truth images, (a₂)-(c₂) segmentations obtained by the manually fine-tuned version, in the same iteration that the autopilot version has converged, (a₃)-(c₃) segmentation results of the autopilot Chan-Vese model.

4. Conclusions

In this work, a novel framework for automated, spatially-adaptive adjustment of regularization and data fidelity parameters is presented and applied for the segmentation of medical images. The proposed framework is based on an isomorphism between these parameters and the eigenvalues of diffusion patterns. Since eigenvalues of diffusion tensors hold vital information associated with localized edges, we embed this information in the amount of diffusion along orthogonal directions by means of spatially-adaptive, entropy ‘heatmaps’, which are able to guide contour evolution.

The proposed framework has been experimentally evaluated on endoscopic as well as mammographic images. The experimental results show that the autopilot version is capable of accelerating contour convergence as well as maintaining a high segmentation quality, comparable to the one obtained by the manually fine-tuned version. It should be noted that, the latter is a cumbersome and time-consuming process which requires technical skills from the end user and generates segmentation results which lack objectivity. Future directions of this work include investigation of the proposed framework on different types of medical image modalities.

Acknowledgements

We would like to thank the General Hospital of Athens “Laiko”, Medical School for the provision of endoscopic data as well as Prof. M. Tzivras and his research group for the provision of the ground truth. This research has been co-financed by the European Union (European Social Fund-ESF) and Greek national funds through the Operational Program “Education and Lifelong Learning” of the National Strategic Reference Framework (NSRF)-Research Funding Program:

Heracleitus II. Investing in knowledge society through the European Social Fund.

5. References

- [1] Y. Rathi, N. Vaswani, A. Tannenbaum and A. Yezzi, "Tracking Deformable Objects Using Particle Filtering for Geometric Active Contours," *IEEE Transactions on Pattern Analysis and Machine Intelligence*, vol. 29, no. 8, 2007, pp. 1470-1475.
- [2] G. Sundaramoorthi, A. Yezzi and A. Mennucci, "Coarse-to-Fine Segmentation and Tracking Using Sobolev Active Contours," *IEEE Transactions on Pattern Analysis and Machine Intelligence*, vol. 30, no. 5, 2008, pp. 851-864.
- [3] K. Zhang, H. Song and L. Zhang, "Active Contours Driven by Local Image Fitting Energy," *Pattern Recognition*, vol. 43, no. 4, 2010, pp. 1199-1206.
- [4] P. Horváth, I.H. Jermyn, Z. Kato and J. Zerubia, "A Higher-Order Active Contour Model of a 'Gas of Circles' and its Application to Tree Crown Extraction," *Pattern Recognition*, vol. 42, 2009, pp. 699-709.
- [5] T.F. Chan and L.A. Vese, "Active Contours Without Edges," *IEEE Transactions on Image Processing*, vol. 10, no. 2, 2001, pp. 266-277.
- [6] Y. Shang, X. Yang, L. Zhu, R. Deklerck and E. Nyssen, "Region Competition Based Active Contour for Medical Object Extraction," *Computerized Medical Imaging and Graphics*, vol. 32, no. 2, 2008, pp. 109-117.
- [7] L. Wang, C. Li, Q. Sun, D. Xia and C.-Y. Kao, "Active Contours Driven by Local and Global Intensity Fitting Energy with Application to Brain MR Image Segmentation," *Computerized Medical Imaging and Graphics*, vol. 33, 2009, pp. 520-531.
- [8] J. Xu, J.P. Monaco and A. Madabhushi, "Markov Random Field Driven Region-Based Active Contour Model (MaRACel): Application to Medical Image Segmentation," in Proc. *International Conference on Medical Image Computing and Computer-Assisted Intervention (MICCAI)*, 2010, pp. 197-204.
- [9] K. Ramudu, G.R. Reddy, A. Srinivas and T.R. Krishna, "Global Region Based Segmentation of Satellite and Medical Imagery with Active Contours and Level Set Evolution on Noisy Images," *International Journal of Applied Physics and Mathematics*, vol. 2, no. 6, 2012, pp. 449-453.
- [10] L. Ma and J. Yu, "An Unconstrained Hybrid Active Contour Model for Image Segmentation," *IEEE 10th International Conference on Signal Processing (ICSP)*, 2010, pp. 1098-1101.
- [11] C. McIntosh and G. Hamarneh, "Is a Single Energy Functional Sufficient? Adaptive Energy Functionals and Automatic Initialization," in Proc. *International Conference on Medical Image Computing and Computer-Assisted Intervention (MICCAI)*, 2007, pp. 503-510.
- [12] E. Erdem and S. Tari, "Mumford-Shah Regularizer with Contextual Feedback," *Journal of Mathematical Imaging and Vision*, vol. 33, 2009, pp. 67-84.
- [13] C. Pluempitwiriyawej, J.M.F. Moura, Y.J.L. Wu and C. Ho, "STACS: New Active Contour Scheme for Cardiac MR Image Segmentation," *IEEE Transactions on Medical Imaging*, vol. 24, no. 5, 2005, pp. 593-603.
- [14] A. Tsai, A. Yezzi, W. Wells, C. Tempany, D. Tucker, A. Fan, W.E. Grimson and A. Willsky, "A Shape-Based Approach to the Segmentation of Medical Imagery Using Level Sets," *IEEE Transactions on Medical Imaging*, vol. 22, no. 2, 2003, pp. 137-154.
- [15] B. Dong, A. Chien, Y. Mao, J. Ye and S. Osher, "Level Set Based Surface Capturing in 3D Medical Images," in Proc. *International Conference on Medical Image Computing and Computer-Assisted Intervention (MICCAI)*, 2008, pp. 162-169.
- [16] D. Tschumperlé and R. Deriche, "Vector-Valued Image Regularization with PDEs: a Common Framework for Different Applications," *IEEE Transactions on Pattern Analysis and Machine Intelligence*, vol. 27, no. 4, 2005, pp. 506-517.
- [17] M.N. Do and M. Vetterli, "The Contourlet Transform: an Efficient Directional Multiresolution Image Representation," *IEEE Transactions on Image Processing*, vol. 14, no. 12, 2005, pp. 2091-2106.
- [18] W.R. Crum, O. Camara and D.L.G. Hill, "Generalized Overlap Measures for Evaluation and Validation in Medical Image Analysis," *IEEE Transactions on Medical Imaging*, vol. 25, no.11, 2006, pp. 1451-1461.
- [19] J. Suckling, J. Parker, D. Dance, S. Astley, I. Hutt, C. Boggis, I. Ricketts, E. Stamatakis, N. Cerneaz, S. Kok, P. Taylor, D. Betal and J. Savage, "The Mammographic Images Analysis Society Digital Mammogram Database," *Experta Medica International Congress Series*, vol. 1069, 1994, pp. 375-378.